FME HighEFF

Centre for an Energy Efficient and Competitive Industry for the Future

Deliverable D3.3_2019.01

Thermal storage for improved utilization of renewable energy in steam production

Delivery date: 2019-10-28

Organisation name of lead partner for this deliverable:

SINTEF Energy Research

HighEFF- Centre for an Energy Efficient and Competitive Industry for the Future is one of Norway's Centre for Environment-friendly Energy Research (FME). Project co-funded by the Research Council of Norway and Industry partners. Host institution is SINTEF Energi AS.		
Dissemination Level		
PU	Public	X
RE	Restricted to a group specified by the consortium	
INT	Internal (restricted to consortium partners only)	

Deliverable number:	D3.3_2019.01
ISBN number:	
Deliverable title:	Thermal storage for improved utilization of renewable energy in steam production
Work package:	3.3
Deliverable type:	Report
Lead participant:	SINTEF Energy Research

Quality Assurance, status of deliverable		
Action	Performed by	Date
Verified (WP leader)	Hanne Kauko	2019-10-28
Reviewed (RA leader)	Trond Andresen	2019-11-05
Approved (dependent on nature of deliverable)*)	Trond Andresen	2019-11-05

*) *The quality assurance and approval of HighEFF deliverables and publications have to follow the established procedure. The procedure can be found in the HighEFF eRoom in the folder "Administrative > Procedures".*

Authors		
Author(s) Name	Organisation	E-mail address
Hanne Kauko	SINTEF Energy Research	Hanne.kauko@sintef.no
Alexis Sevault	SINTEF Energy Research	Alexis.sevault@sintef.no
Gerwin Drexler-Schmid	Austrian Institute of Technology	Gerwin.Drexler-Schmid@ait.ac.at
Anton Beck	Austrian Institute of Technology	Anton.Beck@ait.ac.at

Abstract
This report introduces four different thermal storage technologies suitable for the purposes of steam production and storage: latent heat, molten salt, concrete, and Ruths steam storage. The technologies are compared in the scope of a power-to-heat case study, where electricity from renewable sources with varying price level is to be used for large-scale steam production. Based on this rough initial comparison, it appears that molten salt and latent heat storage are the technologies with the highest potential for large scale steam storage due to the lowest investment costs as well as lowest volume requirement. Latent heat storage is however yet at a lower TRL level, while for the other technologies, suppliers are available. Molten salt storage is a proven technology, applied in several large-scale concentrated solar power systems. Ruths steam storage is widely applied in the process industry to balance for rapid changes in steam demand, but the technology is not suited for large-scale applications with long storage times. Concrete storage is an upcoming technology, with several successful pilot systems commissioned.

Executive summary

This report introduces four different thermal storage technologies suitable for the purposes of steam production and storage: latent heat, molten salt, concrete, and Ruths steam storage. The technologies are compared in the scope of a power-to-heat case study, where electricity from renewable sources with varying price level is to be used for large-scale steam production. To be able to cover the entire steam demand during the high-price period, 10 MWh of storage capacity is required.

Based on this rough initial comparison, it appears that molten salt and latent heat storage are the most potential technologies for large scale steam storage. The estimated payback time of molten salt storage is 1.2 years, while the payback time of latent heat storage is 1.6 years. The payback times for concrete and Ruths steam storage were estimated to 2 and 2.6 years, respectively. The estimated volume requirement of molten salt, latent heat, concrete and Ruths steam storages were 115 000, 140 000, 240 000 and 159 000 m^3, in respective order.

Latent heat storage is however yet at a lower TRL level, while for the other technologies, suppliers are available. Molten salt systems are a proven technology, applied for several commercial large-scale TES systems for concentrated solar power. Ruths steam storage is widely applied in the process industry to balance for rapid changes in steam demand, but the technology is not suited for large-scale applications with long storage times. Concrete storage is an upcoming technology, with several successful pilot systems commissioned.

Molten salt storage possesses however some inherent disadvantages; most of all the high melting point, requiring an auxiliary heating system for all components to prevent the solidification of the salt, also when the system is not in use. A drawback of concrete storage is the varying charge and discharge rate resulting from varying inlet and outlet temperatures. This drawback may also be present in latent heat storage systems due to the varying thermal conductivity with varying degree of solidification. Molten salt storage on the other hand holds constant inlet and outlet temperatures, and a charge and discharge rate that is easy to control by controlling the mass flow.

The choice of the correct TES technology for a specific industrial application is largely dependent on the boundary conditions of the application. A methodology for choosing the correct TES technology, as well as the correct heat-to-power conversion technology, will be developed within the Novel Emerging Concept project CETES – Cost-efficient thermal energy storage for increased utilization of renewable energy in industrial steam production.

Table of Contents

1 Introduction

Steam systems are a part of almost every major industrial process, in nearly all industrial sectors. Steam generation systems were estimated to account for 38 % of global final manufacturing energy use or 44 EJ in 2005 (Banerjee, Gong et al. 2012), corresponding to 9 % of the global final energy consumption. The most important purposes of using steam are heating, drying or concentration, steam cracking, and distillation (Einstein, Worrell et al. 2001). In drying or concentration, steam is used to evaporate water to concentrate solids in a solution, or to dry out a solid product. Cracking is the process of breaking a long chain of hydrocarbons into short ones, i.e., the process of producing lighter fuels, and consists simply of heating steam and fuel together in a high-pressure chamber. Distillation is the process of separating out specific chemicals or fuels out of a complex feedstock.

Steam production is still primarily based on the use of fossil fuels, and all the major industrial energy users devote significant proportions of their fossil fuel consumption to steam production. Although there is a lot of data available for the industrial energy use by sector and energy carrier (e.g. (IEA 2007), (SSB 2018)), there is little knowledge on how large share of the energy consumption is devoted to steam generation. A study carried out in the USA revealed that the share of fossil fuel devoted to steam production is highest in the pulp and paper industry (81 %), followed by food processing industry (57 %), chemicals (42 %), petroleum refining (23 %), and primary metals (10 %) (Einstein, Worrell et al. 2001).

There is thus an urgent demand to develop cost-efficient alternatives for fossil-based steam generation. Steam can be generated by renewable energy either directly with concentrated solar power (CSP), or with electricity from renewable sources by using an electric boiler or a high-temperature heat pump (HTHP). The latter, direct transformation of electrical energy into thermal energy, is referred to as power-to-heat. In this case, thermal energy is produced and stored in times of low electricity prices and is available when required. Power-to-heat is crucial for the energy revolution, as it can replace the use of fossil fuels with renewable energy in the heating sector with rather small changes in the infrastructure. At the same time the security of supply can be increased, because of the quick controllability by interception and use of generation peaks in the grid (Unseld 2015).

In either case, CSP or power-to-heat, thermal energy storage (TES) is a key enabling technology. TES allows higher production of steam when solar heat is available or electricity prices are low, to be stored and utilized upon demand. The focus in this report is thus on TES technologies that may enable improved utilization of renewable energy in steam production. The technologies discussed in this report include (1) steam accumulators, (2) latent heat storage by using phase change materials (PCMs), (3) molten salt storage and (4) concrete storage. The selection of technologies includes both state-of-the-art technologies with potential for further development (steam accumulators and molten salt), as well as technologies with high potential but lower level of maturity (latent heat and concrete storage).

The report is organized as follows. The selected TES technologies are introduced in Chapter 2 with respect to their thermodynamic properties, including examples of their practical application. Chapter 3 presents a comparison of the four technologies in a power-to-heat case study in terms of cost, size, safety and environment, as well as feasibility. Chapter 4 concludes the report. The report focuses on the production and use of steam in industrial processes; thus, steam generation for power production is not included. Furthermore; this study does not cover the technologies suited for power-to-heat conversion. The use of high-temperature heat pumps for steam production has been discussed in another project (Gabrielii, Schlemminger et al. 2018).

2 Thermal storage technologies

2.1 Steam accumulators

One of the most commonly used and proven storage technologies for thermal energy is the Ruths steam accumulator, shown in Figure 2-1, which is a pressure vessel containing a two-phase mixture of liquid and steam. Today, steam accumulators are used e.g. in paper, metal, food and chemical industries. The possibility for integration of steam storages as a buffer in solar thermal systems has also been considered (Steinmann and Eck 2006). Fabrizio, Gay et al. (2011) mentioned the integration of steam storages in industrial food processes and the possibility to cover short-term peak loads. The stored steam is mainly used for heating, cleaning, drying and pressing. In industrial applications, often several Ruths steam accumulators are combined to a storage line.

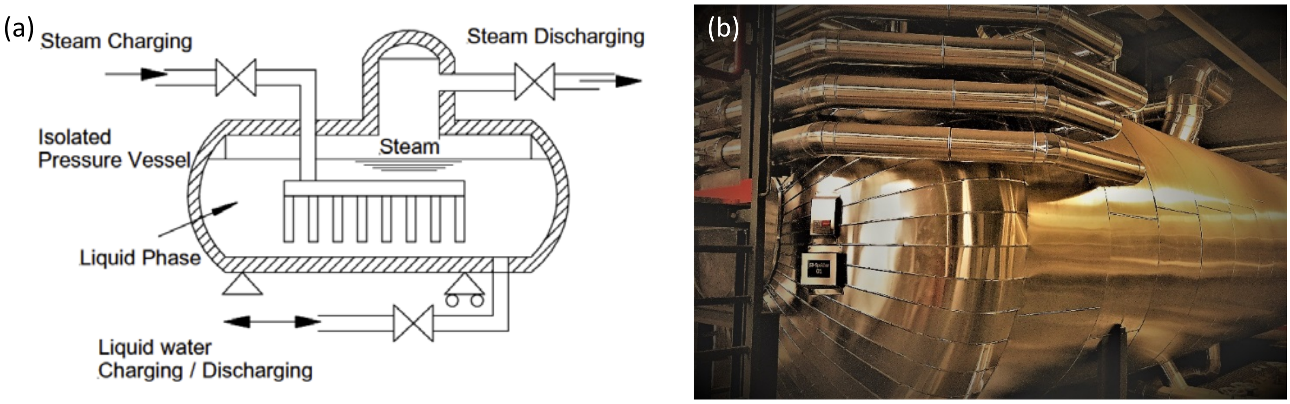

Figure 2-1 (a) Scheme of a Ruths steam storage according to Steinmann and Eck (2006). (b) Industrial steam accumulator (AIT, Voestalpine AG).

2.1.1 Thermodynamic properties

This vessel is charged and discharged directly with steam. Thus, the storage medium is equal to the heat transfer medium, and high heat transfer rates are obtained, determined by the charging/discharging rate of steam. During charging of the storage tank, the incoming steam partly condenses, which leads to an increase in the liquid filling level and, also in pressure and temperature. During discharge, the saturated steam contained in the storage tank is removed, which causes a decrease of pressure, temperature and liquid filling level to maintain a thermodynamic equilibrium in the vessel. (Buschle, Steinmann et al. 2006, Steinmann and Eck 2006, Fabrizio, Gay et al. 2011, Goldstern 2013).

Storage capacity is not only determined by storage size but also by the temperature range of operation. This means that the resulting pressure difference inside the vessel has a big impact on specific storage capacity. However, with increased maximal pressure also higher requirements regarding mechanical and thermal stresses are imposed on the pressure vessel. Typical storage volumes go up to 300 m³. Maximum charging/discharging rates of steam accumulators depend on the piping dimensions. In general, high heat loads can be realized. Steam accumulators can be used as buffer storage as they can provide the stored capacity within a short time of 5 to 10 minutes (Steinmann and Eck 2006).

2.1.2 Practical application

If a thermal storage is to be integrated into an existing energy system, the requirements, such as storage time, storage capacity charging and discharging time, must be defined in advance. The appropriate design of thermal energy systems strongly depends on the process requirements for steam supply. If the storage system is also to be used to exploit opportunities to participate in energy markets, requirements become even more complex.

2.2 Phase change materials

Latent heat storages offer large energy densities without high pressures as in steam accumulators or pressurized water tanks. In latent heat storage, heat is stored as the latent heat of phase change of the storage medium: melting or vaporization. In vaporization, the change in density is large, due to which the solid-liquid phase change process is preferred in TES applications. Latent heat is unique in that the temperature of the material remains nearly constant during the phase change process. An overview on PCMs for applications in the industry can be found in previous HighEFF deliverables, (Foslie, Knudsen et al. 2017) and (Drexler-Schmid and Kauko 2017).

Compared to sensible heat storage materials, PCMs can store or release between 5 and 14 times more energy per unit volume (Sharma, Tyagi et al. 2009, Ibrahim, Al-Sulaiman et al. 2017), depending on the material and selected temperature difference. In Figure 2-2 an overview of volume specific phase change enthalpies for different groups of materials with a phase change temperature above 100°C is presented. Latent heat storages offer an interesting option for industrial applications, as the amount of required storage material is significantly reduced compared to a sensible storage and thus also the required storage volume is decreased.

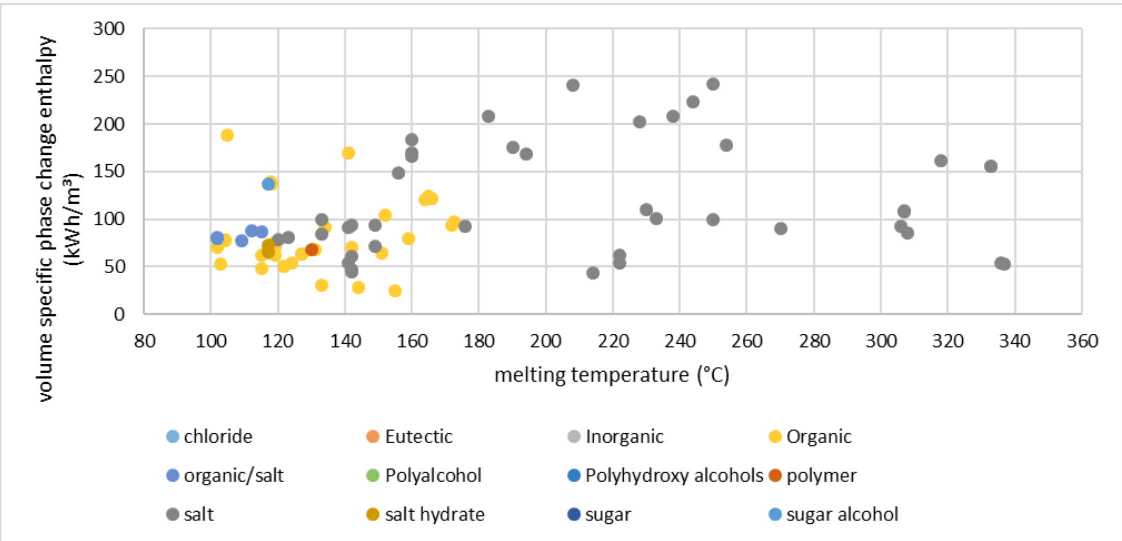

Figure 2-2: Survey of PCMs with melting temperatures above 100°C

2.2.1 Thermodynamic properties

Table 2-1 summarizes the main thermodynamic properties of the most common groups of PCMs. For high-temperature applications (from 120 to 1000 °C), the best suited PCMs available are those based on inorganic salts and metal alloys. A comprehensive overview on the available materials in these groups has been given in (Kenisarin 2010). Regarding salts and their mixtures, Kenisarin (2010) concludes that despite a considerable quantity of studies devoted to studying these materials, only a few compositions have passed all examinations and testing cycles necessary for producing a commercial product. Another disadvantage with salts is their low heat conductivity, and the solutions available to overcome this issue is still limited. At the same time, it seems that the use of phase change metal alloys for high-temperature TES has been underestimated by researchers though they are superior to salts in many respects.

Table 2-1 Thermal properties of different groups of PCMs.

	Melting temperature [°C]	Latent heat [kJ/kg]	Thermal conductivity (solid phase) [W/(m·K)]	Costs	Source
Organic PCMs (paraffins fatty acids, polymers)	0-250	100-200	0.1-0.7	From 4.5 EUR/kWh for fatty acids to >25 EUR/kWh for less common PCMs	(Da Cunha and Eames 2016)
Inorganic PCMs (salts and salt hydrates)	10 to 900	200-900	1-5	1.1 to 4.5 EUR/kWh	(Kenisarin 2010, Fleischer 2015, Da Cunha and Eames 2016)
Metallic	400 to >1000	200-600	160 ($AlSi_{12}$)	-	(Kenisarin 2010)
Eutectic PCMs	For 130 up to 1250 for eutectic mixtures of inorganic salts			1.6 to 34 EUR/kWh	(Da Cunha and Eames 2016)

A problem with PCMs is the low thermal conductivity and the limited heat transfer between the heat transfer fluid (HTF) and the PCM (Laing, Bauer et al. 2013, Ibrahim, Al-Sulaiman et al. 2017). In recent years, the development of methods to increase the heat transfer between the heat transfer medium and PCM, thus improving the performance of the latent heat TES, has been a major research topic. Common methods for heat transfer enhancement can be found in e.g. (Fleischer 2015).

In Figure 2-3, a cost analysis for two different combinations of heat transfer enhancement and PCM material is presented. The studied PCMs were eutectic salt mixtures $LiNO_3$-NaCl and $NaNO_3$-KNO_3, and the considered heat transfer enhancements were aluminum fins and graphite flakes (Figure 2-3 (b)). For this analysis it was assumed that the PCM storage is charged and discharged using steam as a heat transfer medium. The storage was charged using steam at 250 °C and for discharging, pressurized water at 200 °C was evaporated. A charging/discharging cycle of 24 hours was considered, e.g., with a 2-hour charging duration, discharging was assumed 22 hours. The material properties for $LiNO_3$-NaCl/$NaNO_3$-KNO_3 applied in the calculations were:

- melting temperature 214/220 °C;
- volume specific phase change enthalpy 334/105 kJ/kg;
- heat conductivity 0.73/1.35 W/(m·K);
- material costs 2/0.5 €/kg.

The costs for aluminum fins were assumed to be 7 €/kg, the costs for graphite flakes 1€/kg, and the costs for steel pipes 6 €/kg. Equal heat transfer coefficients (500 W/m²K) between the heat transfer fluid and PCM were assumed for both charging and discharging.

In Figure 2-3 (a), resulting specific storage costs are presented. The reason that there is a maximum for kWh/€ storage costs at a charging duration lower than 12 hours is due to the fact that the driving temperature difference between the heat transfer fluid (saturated steam, evaporating water) and the melting PCM is higher during charging for both PCM materials. Also, even though LiNO3-NaCl is more expensive, its higher energy density results in lower costs for heat transfer enhancement and thus in lower overall costs for the system. However, the storage costs strongly depend on the PCM and heat transfer enhancement used and need to be evaluated for each application individually as a lot of factors need to be considered.

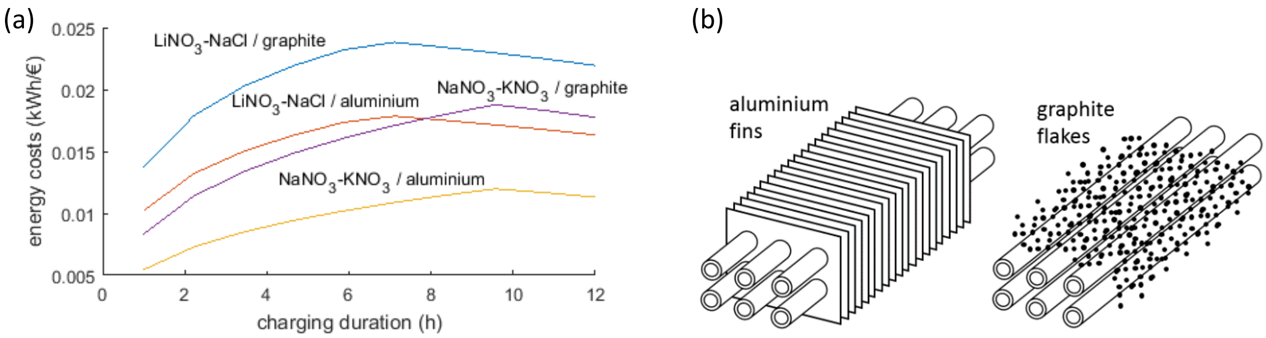

Figure 2-3: (a) Specific energy costs for two different PCMs and two different heat transfer enhancements, illustrated in (b).

2.2.2 Practical application

In literature, latent heat storage with water/steam as a heat transfer medium is often mentioned in combination with direct steam generation systems (Guo and Zhang 2008, Tamme, Bauer et al. 2008, Ju, Xu et al. 2015). This is due to the fact that both the heat transfer fluid (water/steam) and the PCM undergo phase changes at nearly constant temperature and thus constant temperature differences can be maintained.

In pulp and paper production, steam is employed to produce electricity and in different processes. Zauner, Hofmann et al. (2018) investigated a paper mill where roughly half of the steam extracted from the turbine at 3 bars and 150 °C is used at the papermaking machines. Thus, in the event of paper tearing a large amount of excess steam cannot be utilized and has to be cooled in an auxiliary condenser. Excess steam events occur roughly once a day and last for up to a few hours. They proposed a latent heat storage system capable of storing that energy to generate steam at a later time. When the papermaking machines resume production after a paper tearing event, the system is used to reduce the shutdown periods, increase production capacity and save energy. Schematics of the storage integration is presented in Figure 2-4.

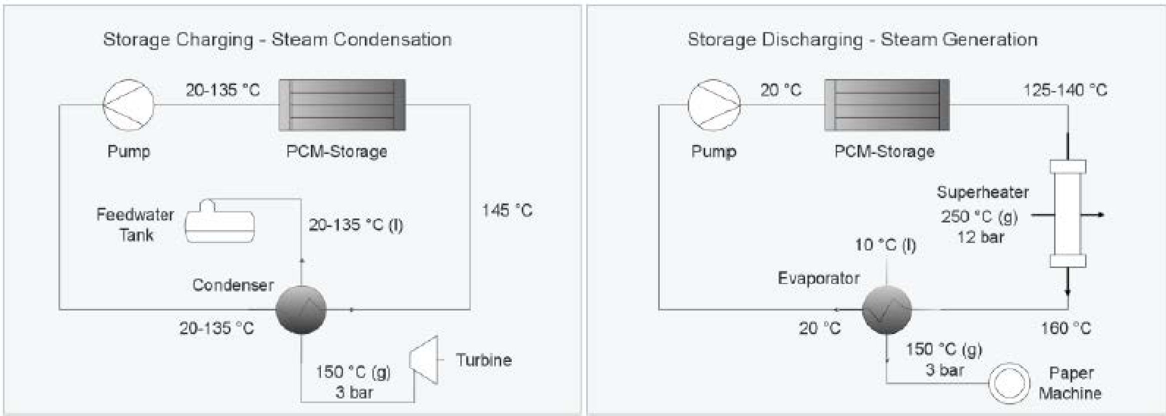

Figure 2-4: Left: Schematics of the system for charging the PCM storage with excess steam in the event of paper tearing. Right: Schematics of generating steam by discharging the storage (Zauner, Hofmann et al. 2018)

A latent heat storage system for direct steam generation to produce electricity was studied by Morisson, Rady et al. (2008). For charging, the steam generated by a solar collector field condenses inside the storage and for discharging water is evaporated inside the storage. As PCM a graphite-salt composite was used to ensure sufficient heat transfer between the heat transfer medium and the heat storage medium. Using a graphite-salt composite (4% graphite) it was possible to significantly increase the effective heat conduction.

Laing, Bauer et al. (2013) presented a latent heat storage for direct steam generation which was tested with different operating modes in a 1 MW test facility. Moreover, a storage system consisting of two sensible and one latent heat storage for direct steam generation power plants was presented by Laing, Bahl et al. (2011). The sensible storage tanks are used for preheating and overheating and the latent heat storage tank for evaporation during discharge mode.

A comparison between different storage technologies for the integration into direct steam generation solar plants was presented by Prieto, Rodríguez et al. (2018). The study showed that for discharging times longer than six hours, a combination of latent heat storage and molten salt storage is preferable to steam storages.

Different combinations of steam accumulators and PCM have also been investigated, for example, through different arrangements of PCM inside the Ruths steam storage pressure vessel (Buschle, Steinmann et al. 2006, Steinmann and Eck 2006, Tamme, Bauer et al. 2008). Another considered approach was using a tube register surrounded by PCM (Buschle, Steinmann et al. 2006, Tamme, Bauer et al. 2008). The tube register was connected to the pressure vessel, which acts as a reservoir and a separator. The tube register arranged outside the pressure vessel provides better results in terms of solidification time than the arrangement at the internal side of the pressure vessel.

2.3 Molten salt

Molten salt storage is the preferred storage technology in CSP applications. It is a proven technology, applied for several commercial large-scale TES systems for CSP, and currently the most applied TES used in electricity generation, with 3.3 GW of installed storage power capacity (2 % of total global electric storage capacity) (IRENA 2017). The specific storage costs are low, and the storage is easily scalable. Further advantages of molten salt include good thermal stability at high temperatures, low vapor pressure, low viscosity, high thermal conductivity, non-flammability and non-toxicity (Pelay, Luo et al. 2017). The low vapor pressure allows storage designs without pressure vessels. Moreover, power in- and output, i.e., the charge and discharge rate are easily controlled by controlling the mass flow (Barragán and Schmitz 2015). A major difficulty with molten salts is unwanted freezing during operation due to high melting temperatures, requiring auxiliary heating for the storage tanks and piping. Salt mixtures with low melting temperature are under development (Bauer, Breidenbach et al. 2012).

Common candidates for molten salt storage in CSP plants are so-called Solar Salt, Hitec and HitecXL (Kearney, Kelly et al. 2003, Bauer, Breidenbach et al. 2012, Pelay, Luo et al. 2017). This report discusses and compares the properties of these three salts, as well as Yara MOST, a new ternary salt mixture developed by Yara (Yara 2019).

2.3.1 Thermodynamic properties

Table 2-2 shows the composition and the thermodynamic properties of the four molten salt alternatives mentioned above: Solar Salt, Hitec, HitecXL and Yara MOST. From these salts, HitecXL possesses the lowest melting point, while Yara MOST has clearly the highest specific heat capacity and lowest viscosity. Moreover, Yara MOST has higher density than the other salts, reducing the required storage volume.

Table 2-2 Composition and thermodynamic properties of molten salts commonly used for CSP applications (Kearney, Kelly et al. 2003) as well as the Yara MOST salt (Doppelbauer 2018). Price data for solar salt and Hitec was retrieved from Alibaba.com.

	Solar Salt	Hitec	HitecXL	Yara MOST
Composition				
$NaNO_3$	60	7	7	15
KNO_3	40	53	45	43
$CaNO_3$				42
$NaNO_2$		40		
$Ca(NO_3)_2$			48	
Melting point [°C]	222	142	120 (130?)	130 - 135
Thermal decomposition [°C]	600	535	500	≥ 525
Density [kg/m^3] at 300°C	1899	1640	1992	2137 ± 50
C_p [J/(kgK)] at 300°C	1495	1560	1447	2100 ± 75
Viscosity [mPa·s] at 300°C	3.26	3.16	6.37	2.1 ± 0.1
Thermal conductivity [W/mK]	0.45	0.48		-
Price [€/kg]	0.07-0.91	0.91-1.37	-	0.77

2.3.2 Practical application

The only commercially available molten salt storage concept for large CSP plants at present is a two-tank storage system, consisting of two tanks filled with molten salt at different temperature and fill levels (Bauer, Breidenbach et al. 2012). This system can be either direct or indirect (Figure 2-5). In a direct system the salt is both the storage medium and the HTF; while in an indirect system a separate HTF is used, exchanging heat with the storages.

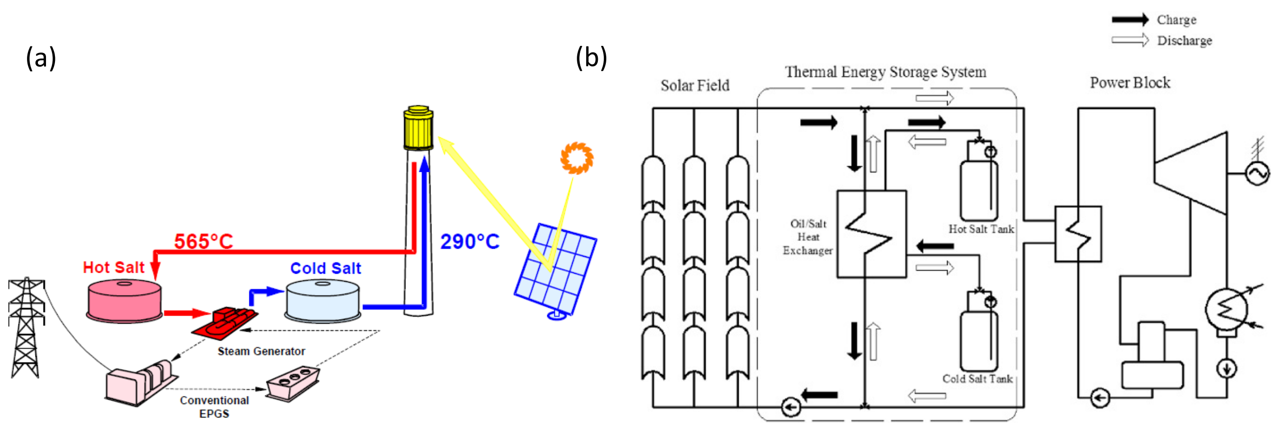

Figure 2-5 (a) Two-tank direct (Pacheco, Bradshaw et al. 2002) and (b) indirect storage system (Li, Xu et al. 2017).

A direct system allows higher solar field outlet temperatures as well as considerably lower system costs as an extra heat exchanger step is avoided (Kearney, Kelly et al. 2003). Salt may also be less expensive and more environmentally benign than other common HTFs applied in CSP systems. Moreover, the temperature difference between the hot and cold tank may be higher in a direct system, reducing the required storage volume and hence system costs (Bauer, Breidenbach et al. 2012). On the other hand, using salt as the HTF requires innovative freeze protection concepts owing to the high melting point of salts, and more expensive materials in the heat transfer system due to possibly higher fluid temperatures. Nevertheless, in a comparison between direct and indirect systems carried out by NREL, a direct system using salt as the HTF and storage medium showed the lowest levelized electricity costs (Kearney, Kelly et al. 2003).

An alternative to the two-tank storage is a single-tank storage system, where a thermal divider plate is used to separate the hot and cold salt. In such configuration, no pipes and pumps are needed to transport the salt between two storage tanks, allowing significantly reduced system costs. There is thus great interest for the development of single-tank storage systems, and some successful demo units are already in operation (DLR 2017, HelioCSP 2017).

Salts are corrosive at high temperatures. Sandia National Laboratories has carried out corrosion test for high temperature alloys (two stainless steel alloys, nickel-chromium alloy and a nickel-chromium-tungsten-molybdenum alloy) with solar salt (Kruizenga, Gill et al. 2013). The results show low corrosion at temperatures of 400 and 500 °C, however significant corrosion at higher temperatures (680 °C). At higher temperatures, significant amounts of alloy elements (chromium, tungsten, etc.) were dissolved in the salt. Tests carried out with Hitec show that equipment of plain carbon steel is satisfactory with temperatures up to 450°C, however more resistant alloys are recommended at higher operation temperatures (Coastal Chemical Co.).

The biggest hazard in the usage of molten salts is related to the high temperatures. Sodium nitrate, contained in all the suggested salts, is a strong oxidizer, and contact with other material may cause fire, and it can cause irritation.

2.4 Concrete

Originally used for thermal management in buildings, TES using concrete in solid state is expected to become an increasingly popular technology for large scale high-temperature TES due to its relatively low cost, easy maintenance, potential for recycling and high heat capacity (John, Hale et al. 2013). The Norwegian company EnergyNest AS[1] produces modular concrete TES units with heat storage capacity from 0.1 MWh to several GWh with typical operational temperature range from 150 °C to 400 °C. Among the challenges with high-temperature concrete TES, the most critical ones are uncontrolled vapor pressure build-up and thermal stress between steel tubes and concrete.

2.4.1 Thermodynamic properties and operational parameters

Thermodynamic and operational data parameters are taken from cited references from EnergyNest and the EnergyNest website[1]. To the authors' knowledge, the Norwegian company is the only one to provide a close-to-commercial technology for high-temperature TES using concrete as the storage medium.

[1] Energy Nest - www.energy-nest.com

Table 2-3: Thermodynamic properties and thermal performance parameters of high-temperature Concrete TES.

Parameter	Value
Temperature range [°C]	150 – 450
Thermal conductivity [W/(m·K)] @ 400 °C	1.64
Heat storage density [kWh/m^3]	24.3 - 43.3
Heat transfer fluid	Thermal oil, water/steam
Design pressure [bar]	160 - 180
Typical footprint [kWh/m^2 for large installations]	364.7
Durability in terms of number of thermal cycles	10 000 – 20 000 (up to 50 years - successfully tested with 280 cycles)
Thermal response time	7 s to 1h
Typical heat loss per 24h [% of stored heat]	2
Cost of storage medium [EUR/kWh$_{th}$]	30-60
Maintenance cost	Very low (no moving parts except valves and pump)
TRL level (2019)	6
Safety & Environment	Storage medium non-toxic and non-corrosive

2.4.2 Practical application

High-temperature concrete TES is primarily thought for CSP to allow for continuous power production. Figure 2-6 illustrates the integration of concrete TES in a CSP plant. However, the scalability and operational temperature range of concrete TES make it a promising candidate technology to enhance the utilization of renewable energy in industrial steam production.

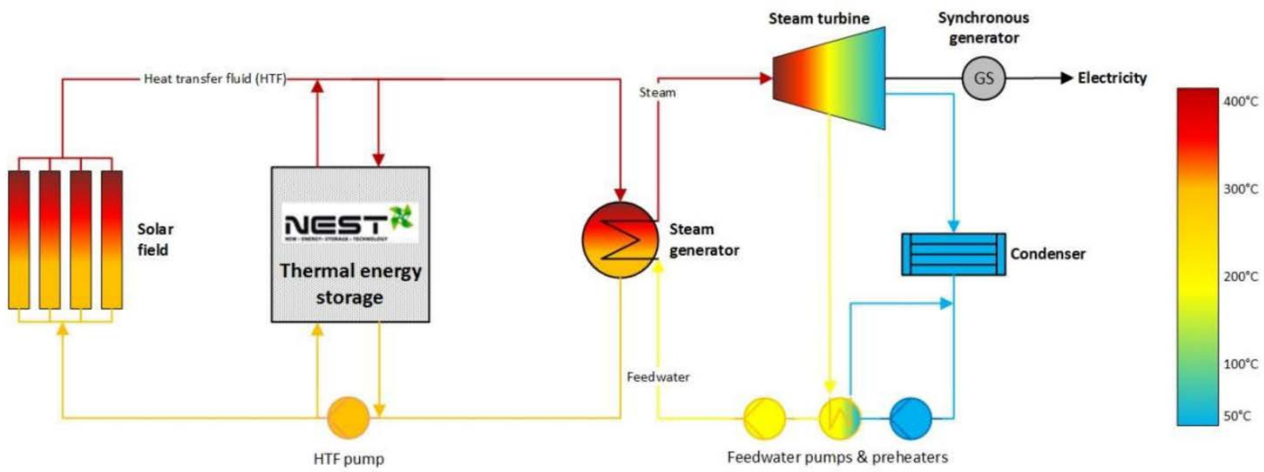

Figure 2-6: Integration of EnergyNest TES unit in CSP plant using synthetic oil as HTF (Bergan and Greiner 2014).

Some of the first concepts of steel pipe heat exchangers built in concrete as high-temperature TES medium (cf. Figure 2-7) were investigated by DLR (Germany) with a 474 kWh$_{th}$ experimental pilot (25.6 kWh/m^3) operating at up to 400 °C (Laing, Steinmann et al. 2007, Laing, Lehmann et al. 2008, Laing, Bahl et al. 2011). They emphasized the critical issue of heating up concrete for the first time up to 400 °C: most of the water contained in the concrete evaporates and eventually yield a vapor pressure build-up in the concrete. If the vapor pressure is not controlled and exceeds a critical value, serious structural damages occur. Therefore, the first major innovation with concrete as high-temperature storage medium was to achieve sufficient permeability of the vapor to avoid vapor pressure build-up. Another challenge was to address the mismatch of the thermal expansion between the steel tube and the concrete. If the steel tubes expand more than the concrete, the concrete may break, which critically impacts the effective thermal conductivity of the storage medium. To limit the longitudinal and radial stress in the tubing to an acceptable level, a compressible, friction-reducing, thermally conductive material was installed between tubes and concrete.

Figure 2-7: Tube register and collectors before pouring heat storage concrete (Laing, Bahl et al. 2011).

Several pilots have also been tested at University of Arkansas (Skinner, Brown et al. 2011, Skinner, Strasser et al. 2013) with successful operations up to 390 °C. Further tests at higher temperature, up to 500 °C, proved successful using an interface material between the steel pipes and the concrete medium, even though micro-cracks appeared in the concrete.

EnergyNest AS demonstrated a 4 x 250 kWh_{th} TES pilot unit at Masdar Institute of Science & Technology Solar Platform (MISP) (Abu Dhabi – UAE), commissioned in 2015 (Bergan and Greiner 2014, Hoivik, Greiner et al. 2017). The pilot unit is based on individual TES elements using steel U-tubes heat exchangers built in Heatcrete®, as shown in Figure 2-8. Heatcrete® is a special concrete technology developed in collaboration with HeidelbergCement AG[2] (Germany). EnergyNest claims to have addressed the challenge the inherent problem of the low thermal conductivity of concrete through their innovative concrete solution Heatcrete®. The new material provides thermal conductivities of 2.76 W/(m·K) at 25 °C and 1.64 W/(m·K) at 400 °C, which is, respectively, 90 % and 37 % higher than those achieved by DLR (Laing, Bahl et al. 2012, Hoivik, Greiner et al. 2019). They also achieved a higher coefficient of thermal expansion for the concrete, close the one of their steel pipes, to significantly lower the risk associated to structural deformation and thermal stresses through high-temperature cycles in the storage medium.

A drawback of concrete storage is that the outlet temperature of the storage decreases during the discharge and the inlet temperature increases during the charge period, resulting in varying charge and discharge rate (Barragán and Schmitz 2015).

[2] Heidelberg Cement AG (Germany) - http://www.heidelbergcement.com/en

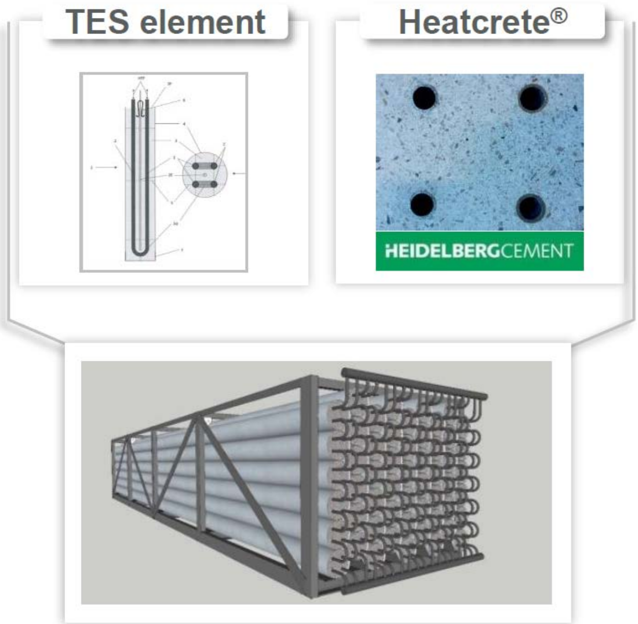

Figure 2-8: TES element developed by Energy Nest. One TES module of 2 m x 2 m x 12 m can store up to 2 MWh_{th} (Greiner 2016).

The four storage modules in the pilot are thermally insulated and operated with thermal oil (Dowtherm A) as HTF at a nominal temperature of 393 °C. Within the two years of operation, hundreds of thermal cycles and thousands of hours of operation were successfully performed. The storage medium also showed neither signs of cracks, nor separation between steel pipes and concrete.

Regarding the modules with 250 kWh_{th} nominal capacity, the specific capacity (including concrete, carbon steel tubes and HTF) was 43.3 kWh/m^3. Typical operation temperatures were 380 °C during charge and as low as 280 °C during discharge. In addition to the high-temperature operations, tests at lower temperatures were also successfully carried out, charging at 240 °C and discharging as low as 165 °C.

As shown in Figure 2-9, the typical response time for the TES system developed by EnergyNest for large installation is over 1 min for about 10 MW_{th} effect up to several hours for 1 GW_{th} effect. Though the system does not enable frequency regulation in electricity network for example, it allows renewables balancing, excess heat recovery, peak power provision, as well as intra-day and day-to-day time shifting.

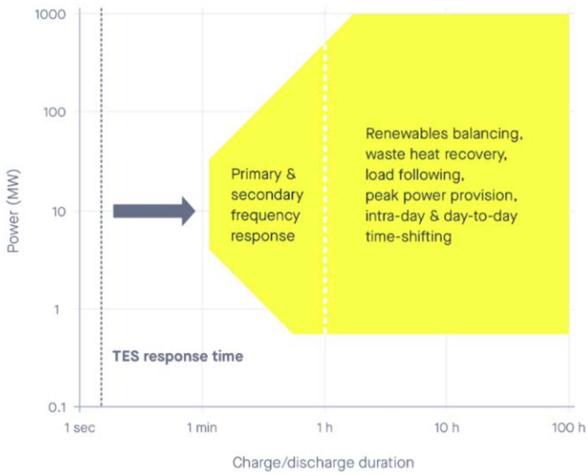

Figure 2-9: EnergyNest[1] operational window.

3 Case study

The four storage technologies introduced in the previous chapter will be compared in a power-to-heat case-study, where renewable electricity is available at variable prices. Thus, the energy source follows the electricity market with two different price levels during a 24-hour period:

- High (between 20:00 and 08:00): 31 €/MWh
- Low (between 08:00 and 20:00): 10 €/MWh

The heat sink is the Bayer process for producing alumina from Bauxite, with a heat requirement of 150 °C. To achieve this and overcome inherent system inefficiencies, the delivery requirement from the storage/steam generator is saturated steam at 200 °C (15.5 bar). The required mass flow rate is 1200 t/h (333 kg/s). The return flow is a mixture of 30% make-up water at 25 °C and 70% return condensate at 95 °C. The properties of the supply and return steam flow are given in Table 3-1. The required heat flow rate can thus be calculated from the mass flow rate and enthalpy difference:

$$\dot{Q} = \dot{m}\left(h_{supply} - h_{return}\right) = 830\ MW$$

Table 3-1 Properties of the steam supplied to and returning from the process.

	Supply	Return	
Share	1	0.7	0.3
Pressure [bar]	15.5	1.0	1.0
Temperature [°C]	200.0	95.0	25.0
State	Sat. steam	Sat. water	Sat. water
Enthalpy [kJ/kg]	2792	398	105
Mixture enthalpy [kJ/kg]		310	
Mixture temperature [°C]		74	

It is assumed that during the low-cost period, an electricity driven steam generator will cover all the steam demand and charge the storage; while in the high-cost period, the storage will cover the entire steam demand. This will give a required storage with a capacity of approximately 10 GWh. Table 3-2 presents the required electricity costs for steam production with and without TES, as well as the resulting savings.

Table 3-2 Daily and yearly electricity costs for steam production with and without TES.

	Per day [M€]	Per year [M€]
Electricity cost without storage	0.81	297
Electricity cost with storage	0.40	145
Savings	**0.41**	**152**

The following sections explain the calculations and assumptions made for calculating the material requirements for each of the four TES technologies. Section 3.5 summarizes the chapter and presents a comparison of the technologies in terms of investment costs, payback time, space demand, HSE as well as operation and maintenance. The scope of the study was to compare the four technologies on as equal basis as possible, and for this reason, heat losses were not considered.

3.1 Ruths steam storage

Figure 3-1 shows the scheme for integration of Ruths steam storage into the steam production system. The main cost drivers for the storage tank are the mass of the steel required for construction and the manufacturing costs. The wall thickness and thus the required steel mass of the pressure vessel are mainly a function of the maximum pressure p_{max} in the storage tank. Increased maximum pressure imposes higher requirements on the mechanical strength of the pressure vessel.

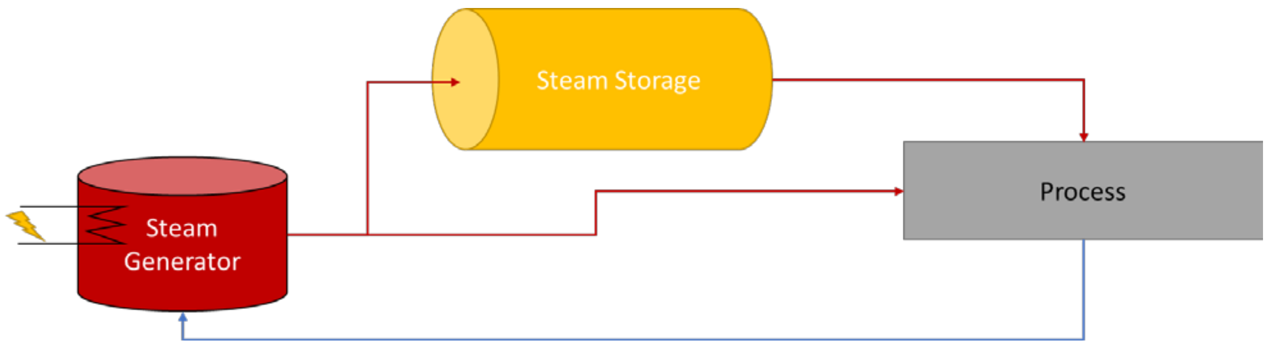

Figure 3-1: Integration scheme for the Ruths steam storage.

The minimum wall thickness s_{min} can be calculated with the so-called boiler formula as follows

$$s_{min} = \frac{p(d+s)}{2\sigma_{steel}(p)} + s_1, \qquad (1)$$

Where σ_{steel} is the maximum permissible stress of the material at a given pressure p, d is the internal diameter of the tank and s is the tank thickness. The safety coefficient s_1 (value given in Table 3-3) is added to ensure that the wall can withstand even minor deviations from the maximum stresses and corrosion and help to obtain physically meaningful solutions for the optimization tasks to determine the cost functions used. The maximum permissible stress determined by means of

$$\sigma_{steel} = \sigma_{steel,yield}\, S, \qquad (2)$$

Where $\sigma_{steel,yield}$ is the yield strength of steel, shown in Figure 3-2 as a function of temperature, and S is a safety coefficient given in Table 3-3.

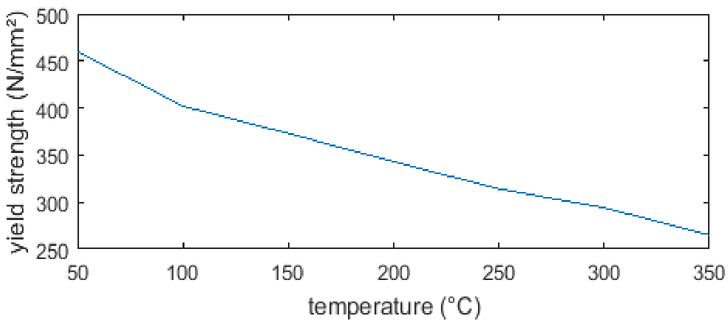

Figure 3-2 Temperature dependence of the yield strength $\sigma_{steel,yield}$ of steel: P460NH / K12202 / WSt460 (LOB GmbH 2009).

Assuming a cylindrical storage tank, steel mass m_{steel} can be specified as the following function of the wall thickness $s_{min}(T)$, the internal diameter and length of the tank l, and the steel density ρ_{steel}.

$$m_{steel} = \left(\left(\frac{d + 2s_{min}}{2}\right)^2 - \left(\frac{d}{2}\right)^2\right)\pi\, l\, \rho_{steel} + 2\left(\frac{d}{2}\right)^2 \pi\, s_{min}\rho_{steel} \quad (3)$$

The costs for the storage can thus be calculated approximately by using specific construction costs k_{steel} for the installed quantity of steel.

$$K_{DS} = m_{steel}k_{steel} \quad (4)$$

The correlation between the storage volume V and the storage parameters d and l is given by the approximation of the pressure vessel by a cylinder by

$$V = \frac{d^2}{4} l\pi. \quad (5)$$

If the storage tank filling level at maximum pressure is also defined, specific storage costs for maximum and minimum storage tank temperatures and different storage tank volumes can be calculated. The maximum energy content for this work was determined by simulating the discharge process with MATLAB and the material data program CoolProp. The minimum storage costs were calculated by minimizing the installed steel mass (Equation (4)) for a given storage volume $\boldsymbol{V}$.

Table 3-3: Material properties and safety coefficients

Steel	**P460NH / K12202 / WSt460**
Density ρ_{steel} [kg/m³]	7850
Safety coefficient S	1.5
Safety coefficient s_1 [m]	0.01

The specific costs for the steam storage determined with the model parameters summarized in Table 3-3 are shown in Table 3-4 for different vessel volumes V and different maximum storage temperatures $Tmax$. The specific material costs used of k_{steel} = 6 €/kg are based on empirical values and include the costs for the manufacture of the pressure vessels. The lowest specific costs are obtained with a maximum temperature of 250 °C and a volume of 300 m³.

Table 3-4: Results for the Ruths steam storage including design parameters and costs

T_{max} [°C]	V [m³]	s_{min} [m]	l/d ratio	Mass [kg]	Capacity [kWh]	Costs [€]	Specific costs [€/kWh]
250	**20**	0.028	3,62	1.53	1,256.97	63,929.68	50.86
	100	0.038	5,05	5.93	6,284.86	270,412.42	43.03
	300	0.047	6,42	15.80	18,854.58	742,915.98	**39.40**
300	**20**	0.045	5,99	2.77	2,372.40	117,583.18	49.56
	100	0.063	8,61	11.64	11,862.01	530,504.35	44.72
	300	0.081	11,12	32.38	35,586.03	1,510,462.55	42.45
350	**20**	0.074	9,65	5.20	3,355.76	224,867.65	67.01
	100	0.107	14,13	23.08	16,778.82	1,055,382.99	62.90
	300	0.138	18,41	65.88	50,336.47	3,067,755.04	60.94

3.2 Phase change materials

In order to investigate the techno-economical suitability of a latent TES, a simple storage model, illustrated in Figure 3-3, was used. Using stationary heat conduction for cylinders, a relation between length and diameter of the steel pipes can be obtained:

$$\dot{Q} = \frac{2\pi\,\lambda\,l\,\Delta T}{\ln\left(\frac{d+2s}{d}\right)} \tag{6}$$

$$s = -\frac{d}{2} + \sqrt{\frac{V_{PCM}}{l\pi} + \frac{d^2}{4}} \tag{7}$$

$$V_{PCM} = \frac{\Delta Q_{req}}{h\,\rho_{PCM}}, \qquad m_{PCM} = V_{PCM}\rho_{PCM} \tag{8), (9}$$

Here, $\dot{Q}$ is the charging/discharging power of the storage at the moment when the phase front of the melting/solidifying PCM is at its maximum. Thus, $\dot{Q}$ is a lower limit of the charging/discharging power. Heat transfer from the heat transfer fluid (evaporating water/condensing steam) to the steel pipes is neglected. The integration of the latent TES into the steam production system is identical with the integration of the Ruths steam storage, shown in Figure 3-1.

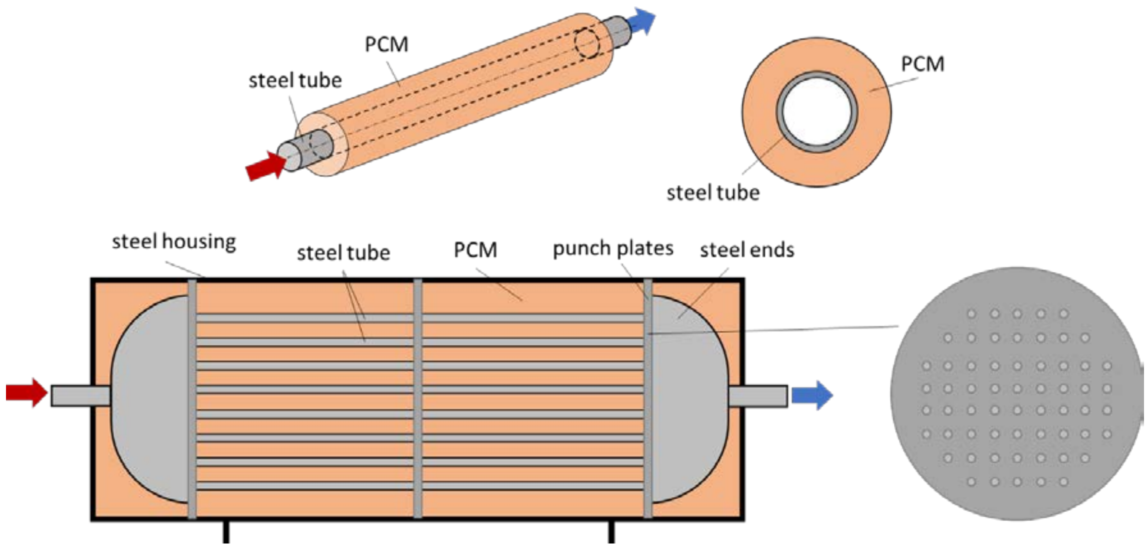

Figure 3-3: Schematic drawing of the PCM storage considered for this case study

Table 3-5: Parameters for cost estimation

Parameter	Value
Welding [€/m] / [€/tube]	1
Housing wall thickness [mm]	3
Carbon steel [€/kg]	1.3
Stainless steel [€/kg]	2
Vessel diameter [m]	1
Vessel length [m]	6
Ends [€]	120
Punch plates [€]	200
PCM [€/kg]	0.5
Average temperature difference [°C]	20

Table 3-6: Specific costs for steel tubes

Tube diameter [mm]	Specific costs [€/m³]	
	Carbon steel	Stainless steel
21.30	2.90	10.00
26.70	3.60	11.00
33.40	5.00	18.00
48.30	7.80	23.00
60.30	9.90	25.00
88.90	16.40	25.00
114.30	24.60	33.00
141.30	35.20	41.00

[3] https://www.dacepricebooklet.com/

Table 3-5 and Table 3-6 show the parameters used for cost estimation and the specific costs for steel tubes. The resulting storage costs for different tube diameters and for both carbon and stainless steel are shown in Table 3-7. The configuration using carbon steel and an outer tube diameter of 21.3 mm yields the lowest storage costs (237.5 M€ / 23.85 €/kWh).

Table 3-7: Resulting storage dimensions and resulting storage costs for various pipe diameters

Tube diameter [mm]	Tube length [km]	PCM thickness [mm]	Total costs including vessels [M€]		Specific costs [€/kWh]		Soccer fields [10,800 m²]	St. Stephan's Cathedrals [82,123 m³]
			Carbon steel	Stainless steel	Carbon steel	Stainless steel		
21.30	19,766	36.91	237.50	390.54	23.85	39.21	8.28	1.71
26.70	17,658	37.47	244.39	388.01	24.54	38.96	8.45	1.74
33.40	15,666	37.97	260.15	477.11	26.12	47.90	8.67	1.79
48.30	12,627	38.67	283.08	489.17	28.42	49.11	9.23	1.91
60.30	10,964	39.00	295.71	476.16	29.69	47.81	9.71	2.01
88.90	8,389	39.44	331.53	420.44	33.29	42.21	10.93	2.26
114.30	6,959	39.64	371.62	448.59	37.31	45.04	12.07	2.49
141.30	5,897	39.76	415.18	469.80	41.68	47.17	13.31	2.75

In Table 3-8, a more detailed analysis for the costs for the steel constructions are presented. The resulting storage costs are additionally shown in Figure 3-4.

Table 3-8: Cost analysis for carbon steel and stainless steel constructions and various tube diameters

	Tube diameter [mm]	Costs [M€]					
		Tubes	PCM	Ends	Punch Plates	Housing	Total
Carbon steel	21.30	57.32	128.06	7.15	27.76	23.80	244.09
	26.70	63.57	128.06	7.30	27.07	24.28	250.28
	33.40	78.33	128.06	7.49	26.57	24.93	265.38
	48.30	98.49	128.06	7.97	26.24	26.52	287.29
	60.30	108.55	128.06	8.39	26.45	27.91	299.36
	88.90	137.59	128.06	9.45	27.81	31.43	334.33
	114.30	171.20	128.06	10.43	29.56	34.70	373.94
	141.30	207.61	128.06	11.50	31.71	38.27	417.15
Stainless steel	21.30	197.66	128.06	7.15	27.76	36.49	397.13
	26.70	194.25	128.06	7.30	27.07	37.23	393.90
	33.40	282.00	128.06	7.49	26.57	38.22	482.34
	48.30	290.43	128.06	7.97	26.24	40.67	493.37
	60.30	274.12	128.06	8.39	26.45	42.79	479.82
	88.90	209.74	128.06	9.45	27.81	48.19	423.24
	114.30	229.65	128.06	10.43	29.56	53.21	450.91
	141.30	241.81	128.06	11.50	31.71	58.69	471.77

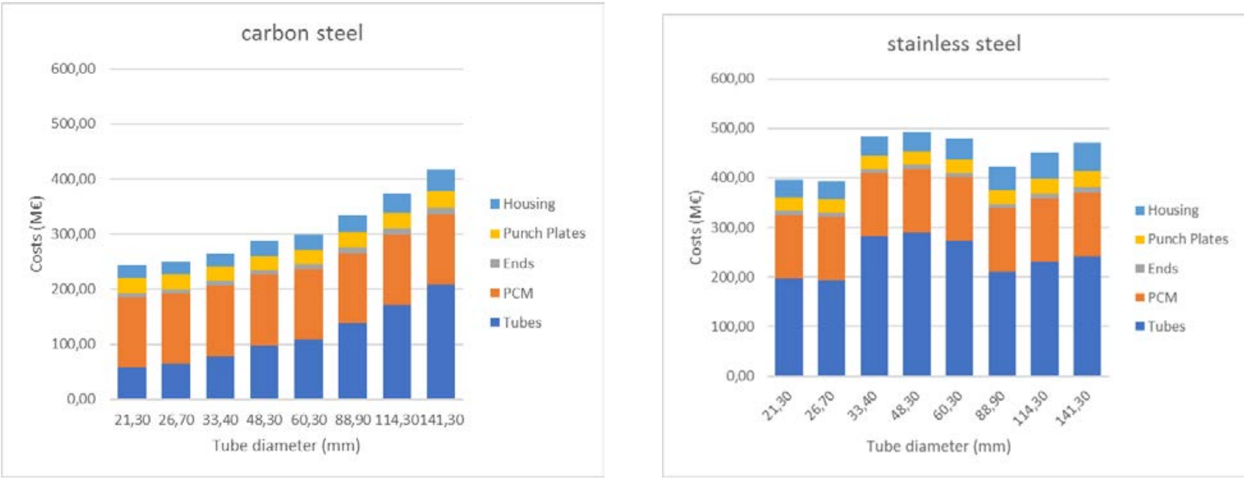

Figure 3-4: Cost analysis of the presented PCM storage configuration for carbon steel and stainless steel

3.3 Molten salt

For the molten salt storage, a two-tank system was considered. Figure 3-5 illustrates the charging and discharging of the storage:

- Charge: cold salt is pumped from the initially full cold tank, through the steam generator heating both salt and the water, and to the hot tank, which is filled up.
- Discharge: hot salt is pumped from initially full the hot tank, through the steam generator where it heats up the water, and to the cold tank.

To be able to deliver steam at a temperature of 200 °C, a temperature of 250 °C was assumed for the hot tank. For the cold tank, a temperature of 180 °C was assumed, considering the melting point of the available salts.

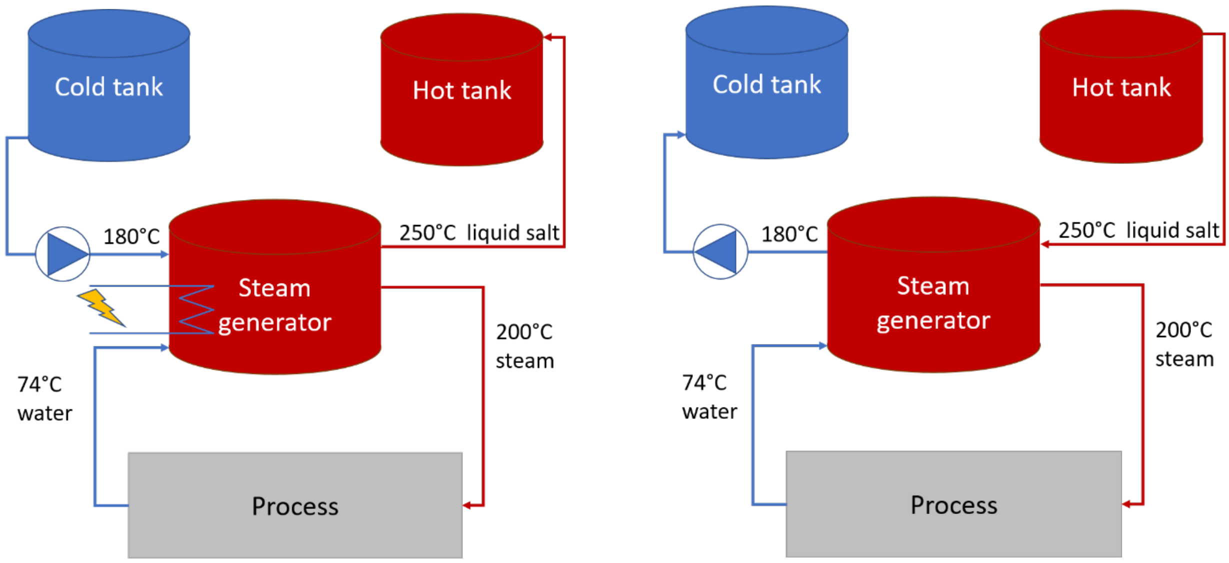

Figure 3-5 Charging (left) and discharging (right) of the molten salt storage system.

From the salts presented in Table 2-2, Hitec and Yara MOST were considered for further the analysis. Solar Salt could not be used in the present application due to its high melting temperature, and Hitec XL was opted out due to its high viscosity and lack of cost data. Table 3-9 shows results for the required salt mass and volume, and consequently the costs, based on the storage requirements and the salt properties presented in Table 2-2. For Hitec, the lower price limit was used. The required amount of salt, and thus the storage material cost, is significantly lower owing to the higher specific heat capacity. Therefore, Yara MOST was chosen as the salt for comparison with the other storage technologies.

Table 3-9 Required amount of salt and the following costs.

	Mass [ton]	Volume [m^3]	Cost [M€]
Yara MOST	244 898	114 599	189
Hitec	329 670	201 018	300

In addition to the storage medium, high capital costs are attributed to the storage tank. According to Glatzmaier (2011), carbon steel tolerates salts at temperatures up to 450 °C and was thus chosen as the storage material. For the tank dimensions, equal aspect ratio was chosen in order to minimize the surface to volume -ratio (thus the material costs) as well as the thermal losses. With $d/l < 1$, the surface to volume ratio increases rapidly, as shown by Figure 3 6. On the other hand, with increasing d/l, the surface area increases rapidly, increasing the thermal losses.

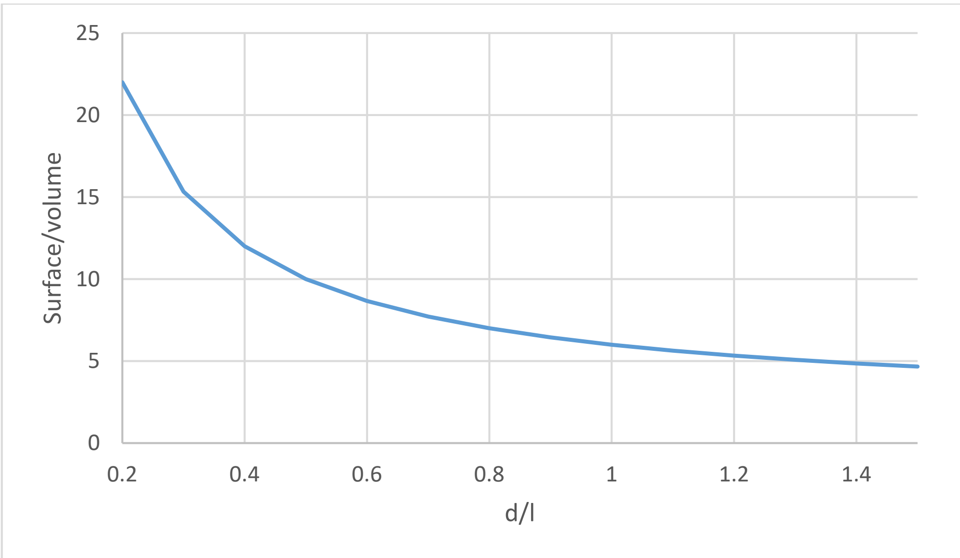

Figure 3-6 Surface-to-volume ratio for a cylindrical tank as a function of the aspect ratio d/l.

When estimating the storage tank costs, the following assumptions were made:

- Cylindrical tank with a size of 1000 m^3 per unit (hot/cold tank), resulting in 115 tanks in total
- Tank thickness of 1 cm (Jonemann 2013).
- Electrical and instrumentation costs = 7 % of total tank costs (Glatzmaier 2011)
- Piping, valves, and fittings costs = 3 % of total tank costs (Glatzmaier 2011)

The material used in calculations was AISI 1045 Medium Carbon Steel, with a density of 7870 kg/m^3 and a price of 642 €/ton. The resulting tank material mass and costs are given in Table 3-10. The required mass of carbons steel was calculated using equation (3), and the costs were calculated using equation (4). When calculating the area requirement, 2 m space between the tanks was assumed.

Table 3-10 Salt storage tank mass, area requirement and costs.

Parameter	Value
Carbon steel mass, total [ton]	1699
Total area requirement [m²]	18 955
Costs tank material [M€]	1.09
Costs piping [M€]	0.03
Costs instrumentation and electrical [M€]	0.08
Total costs [M€]	1.20

The resulting total costs for the tank are roughly 1.2 M€, which is minimal with respect to the storage medium costs of 189 M€. The estimated total storage cost with molten salt TES is thus 190 M€, excluding the costs of circulation pumps.

A disadvantage of molten salt storage is that electricity is required to run the salt circulation pumps, also during the high cost period. Rough calculations were made to estimate the required the required pumping power. Based on the calculations, pumping power was minimal compared to power required for steam production. The power required for running the pumps was thus not considered in the analysis. Another disadvantage of molten salts is the high melting temperature, requiring that all the components in the system are well insulated and equipped with auxiliary heaters in order to prevent freezing of the salt.

3.4 Concrete

Since EnergyNest's concrete TES concept is the closest of its kind to the market, the evaluation of storage costs is based on the price provided by the company, which in the range of 30-60 €/kWh. Provided the large scale of the installation, yielding a lower specific price, the costs for a 10 MWh TES were expected to be in the range of 300-350 M€. The estimated costs of the same amount of regular concrete and stainless steel were only 115 M€; however, as pointed out in section 2.4, plain concrete cannot be used for the purposes of high-temperature TES. Volume and are requirement were calculated based on 2 MW_{th}-modules with a size of 2x2x12 m, stacked by 5 in height (Figure 3-7). The total footprint is thus at least 24 000 m^2 and the total volume requirement is 240 000 m^3. The process integration of concrete TES follows the same approach as the integration of Ruths steam storage and latent heat storage systems.

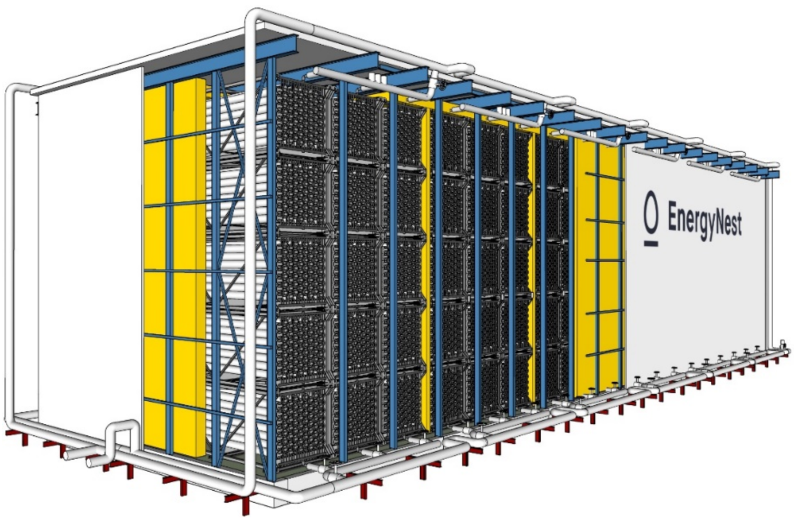

Figure 3-7 Thermal battery system from EnergyNest, made of stacked TES modules.

3.5 Comparison

Table 3-11 presents an overall comparison of the four storage technologies in terms of investment costs, payback time, volume requirement as well as operation and maintenance; and Table 3-12 presents health and safety issues related to these technologies. The payback time was calculated based on the savings in electricity costs for steam production given in Table 3-2. The area requirement is not fully representative due to varying module height; however it gives an indicative area footprint of each storage system.

Table 3-11 Overall comparison of the four storage technologies in the case study.

	Ruths steam storage	Latent heat	Molten salt	Concrete
Volume requirement [m^3]	159 000	140 000	115 000	240 000
Estimated area requirement [m^2] / nr of football fields	52 000 / 4.8 (tank height 4 m)	179 000 / 16.6 (tank height 1 m)	19 000 / 1.8 (tank height 10 m)	24 000 / 2.3 (height 10 m)
Temperature range [°C]	200-250	200-250	180-250	200-250
Total investment cost [M€]	390	240	190	300-350
Included in the investment	Pressure vessel, construction of the vessel	Material costs, welding	Material costs, piping and instrumentation	Full Turn-key facility
Payback time [year]	2.6	1.6	1.2	2-2.3
Operation and maintenance	No special requirements		Electricity required for circulation pumps, auxiliary heating to prevent freezing of salt.	Very little maintenance, lifetime up to 50 years

Table 3-12 Health and safety issues related to the different TES technologies.

	Ruths steam storage	Latent heat	Molten salt	Concrete
Medium	Water	NaNO3-LiNO3 or NaNO3-KNO3	Combination of 2-3 of the following: $NaNO_3$, KNO_3, $CaNO_3$, $NaNO_2$, $Ca(NO_3)_2$	Concrete-cement (Calcium-oxide-based components)
Toxicity	none	H315: causes skin irritation and eyes H319: Causes serious eye irritation H335: May cause respiratory irritation	$NaNO_3$ & KNO_3: can cause eye and skin irritation, as well as respiratory irritation $CaNO_3$: Harmful if swallowed, causes serious eye damage	None, possibly recyclable

Pressure/ Temperature	Large volumes under high pressure and temperature	Small volumes under high pressure	Large volumes under high temperature	Large volume under high temperature
Flammability	Non-flammable	Non- flammable (oxidizer) H272: May intensify fire; oxidizer	Non-flammable but strong oxidizer; enhances combustion of other substances.	Non-flammable
Corrosion	Yes, long term experience available	Yes, no long-time experience	Corrosive at high temperatures (>400-500°C), long term experience available	No, long-lasting and stable structure

4 Summary and conclusions

This report has introduced four different thermal storage technologies suitable for the purposes of steam production and storage: latent heat, molten salt, concrete, and Ruths steam storages. The technologies were compared in the scope of a power-to-heat case study, where electricity from renewable sources with varying price level is to be used for large-scale steam production. To be able to cover the entire steam demand during the high-price period, 10 MWh of storage capacity is required.

In this comparison, molten salt comes out as the winner, with the lowest investment costs as well as lowest volume requirement. The estimated payback time of molten salt storage is 1.2 years, while the payback time of latent heat storage, taking the second place, is 1.6 years. The payback times for concrete and Ruths steam storages were estimated to 2 and 2.6 years, respectively. The estimated volume requirement of molten salt, latent heat, concrete and Ruths steam storages were 115 000, 140 000, 240 000 and 159 000 m^3, in respective order. The cost for the concrete storage was obtained from the supplier, covering the costs for a full turn-key facility, while for the other storage technologies, only material and instrumentation costs were considered. Nevertheless, based on this rough initial comparison, it appears that molten salt and latent heat storages are the technologies with highest potential for large scale steam storage.

From the four TES technologies, latent heat storage is yet at a lower TRL level, while for the other technologies, suppliers are available. Molten salt systems are a proven technology, applied for several commercial large-scale TES systems for CSP. Ruths steam storage is widely applied in the process industry to balance for rapid changes in steam demand, but the technology is not suited for large-scale applications with long storage times. Concrete storage is an upcoming technology, with several successful pilot systems commissioned.

Molten salt storage possesses however some inherent disadvantages; most of all the high melting point, requiring an auxiliary heating system for all components to prevent the solidification of the salt, also when the system is not in use. Moreover, at high temperatures the material quality of containing vessels, pipes and pump needs to be carefully considered. Concrete storage is superior to molten salt storage in these aspects, with safe, reliable and maintenance free materials and components. A drawback of concrete storage is, apart from the rather high space requirement, the varying charge and discharge rates resulting from varying inlet and outlet temperatures. This drawback may also be present in latent heat storage systems due to the varying thermal conductivity with varying degree of solidification. Molten salt storage on the other hand holds constant inlet and outlet temperatures, and a charge and discharge rate that is easy to control by controlling the mass flow.

Nevertheless, the choice of the correct TES technology is largely dependent on the application and its boundary conditions. A methodology for choosing the correct TES technology, as well as the correct heat-to-power conversion technology, will be developed within the Novel Emerging Concept project CETES – Cost-efficient thermal energy storage for increased utilization of renewable energy in industrial steam production.

5 References

Banerjee, R., Y. Gong, D. Gielen, G. Januzzi, F. Maréchal, A. McKane, M. Rosen, D. van Es and E. Worrell (2012). "Energy end-use: industry." Gobal Energy Assessment-Toward a Sustainable Future: 513.

Barragán, J. and M. Schmitz. (2015). "Heatcrete or Molten Salt?" Retrieved 21.10.2019, from http://analysis.newenergyupdate.com/csp-today/technology/heatcrete-or-molten-salt.

Bauer, T., N. Breidenbach, N. Pfleger, D. Laing and M. Eckand (2012). Overview of molten salt storage systems and material development for solar thermal power plants. Proceedings of the 2012 National Solar conference for (SOLAR 2012), Denver.

Bergan, P. G. and C. J. Greiner (2014). "A New Type of Large Scale Thermal Energy Storage." Energy Procedia **58**: 152-159.

Buschle, J., W.-D. Steinmann and R. Tamme (2006). Latent heat storage for process heat applications. Proceedings of the 10th International Conference on Thermal Energy Storage ECOSTOCK, Atlantic City, NJ, USA.

Coastal Chemical Co. HITEC® Heat Transfer Salt.

Da Cunha, J. P. and P. Eames (2016). "Thermal energy storage for low and medium temperature applications using phase change materials–a review." Applied Energy **177**: 227-238.

DLR. (2017). "DLR inaugurates its Test Facility for Thermal Energy Storage in Molten Salt." Retrieved 24.4.2019.

Doppelbauer, G. (2018). Yara MOST - Ternary salt mix as HTF and TES, Yara International.

Drexler-Schmid, G. and H. Kauko (2017). High-temperature phase change material thermal storage for components and cycles, FME HighEFF.

Einstein, D., E. Worrell, M. Khrushch and L. Berkeley (2001). Steam Systems in Industry : Energy Use and Energy Efficiency Improvement Potentials, Lawrence Berkeley National Lab (LBNL), Berkeley, CA (United States)**:** 535–547.

Fabrizio, E., P. Gay and D. RICAUDA AIMONINO (2011). Modelling of Steam Storage Vessels for Batch Processes in Food Plants. Proceedings.

Fleischer, A. S. (2015). Thermal energy storage using phase change materials: fundamentals and applications, Springer.

Foslie, S., B. R. Knudsen, O. Stavset and C. Schlemminger (2017). Industrial energy storage: State-of-the-art report with focus on thermal energy storage, FME HighEFF.

Gabrielii, C., C. Schlemminger and M. Bantle (2018). Thermal upgrading by high temperature heat pump - Case study Hydro Aluminium AS, SINTEF.

Glatzmaier, G. (2011). Developing a cost model and methodology to estimate capital costs for thermal energy storage, National Renewable Energy Lab.(NREL), Golden, CO (United States).

Goldstern, W. (2013). Dampfspeicheranlagen: Bau, Berechnung und Betrieb industrieller Wärmespeicher, Springer-Verlag.

Greiner, C. (2016). Høy-temperatur termisk energilager. Bellona Seminar energilagring, August 2016, EnergyNest.

Guo, C. and W. Zhang (2008). "Numerical simulation and parametric study on new type of high temperature latent heat thermal energy storage system." Energy Conversion and Management **49**(5): 919-927.

HelioCSP. (2017, 26.6.2017). "Single-tank molten salt receiver demo for concentrated solar power successful in Masdar City." Retrieved 26.4.2019, from http://helioscsp.com/single-tank-molten-salt-receiver-demo-for-concentrated-solar-power-successful-in-masdar-city/.

Hoivik, N., C. Greiner, J. Barragan, A. C. Iniesta, G. Skeie, P. Bergan, P. Blanco-Rodriguez and N. Calvet (2019). "Long-term performance results of concrete-based modular thermal energy storage system." (Submitted).

Hoivik, N., C. Greiner, E. B. Tirado, J. Barragan, P. Bergan, G. Skeie, P. Blanco and N. Calvet (2017). "Demonstration of EnergyNest thermal energy storage (TES) technology." **1850**(1): 080011.

Ibrahim, N. I., F. A. Al-Sulaiman, S. Rahman, B. S. Yilbas and A. Z. Sahin (2017). "Heat transfer enhancement of phase change materials for thermal energy storage applications: A critical review." Renewable and Sustainable Energy Reviews **74**: 26-50.

IEA (2007). Tracking industrial energy efficiency and CO2 emissions, International Energy Agency. **34:** 1-12.

IRENA (2017). Electricity storage and renewables: Costs and markets to 2030. Abu Dhabi, International Renewable Energy Agency (IRENA).

John, E., M. Hale and P. Selvam (2013). "Concrete as a thermal energy storage medium for thermocline solar energy storage systems." Solar Energy **96**: 194-204.

Jonemann, M. (2013). Advanced thermal storage system with molten salt, NREL.

Ju, X., C. Xu, X. Li, X. Du and Y. Yang (2015). "Numerical analysis of thermal storage performance with high-temperature phase change materials operated by condensing steam." Solar Energy **117**: 213-223.

Kearney, D., B. Kelly, R. Cable, N. Potrovitza, U. Herrmann, P. Nava, R. Mahoney, J. Pacheco, D. Blake and H. Price (2003). Overview on use of a Molten Salt HTF in a Trough Solar Field. NREL Parabolic Trough Thermal Energy Storage Workshop.

Kenisarin, M. M. (2010). "High-temperature phase change materials for thermal energy storage." Renewable and Sustainable energy reviews **14**(3): 955-970.

Kruizenga, A. M., D. D. Gill, M. LaFord and G. McConohy (2013). "Corrosion of High Temperature Alloys in Solar Salt at 400, 500, and 680 C." Albuquerque: Sandia National Laboratories. SAND2013-2526.

Laing, D., C. Bahl, T. Bauer, M. Fiss, N. Breidenbach and M. Hempel (2012). "High-Temperature Solid-Media Thermal Energy Storage for Solar Thermal Power Plants." Proceedings of the IEEE **100**(2): 516-524.

Laing, D., C. Bahl, T. Bauer, D. Lehmann and W.-D. Steinmann (2011). "Thermal energy storage for direct steam generation." Solar Energy **85**(4): 627-633.

Laing, D., T. Bauer, N. Breidenbach, B. Hachmann and M. Johnson (2013). "Development of high temperature phase-change-material storages." Applied Energy **109**: 497-504.

Laing, D., D. Lehmann and C. Bahl (2008). Concrete storage for solar thermal power plants and industrial process heat IRES III 2008, 3rd International Renewable Energy Storage Conference, 24.-25.11.2008, Berlin.

Laing, D., W.-D. Steinmann, M. Fiß, R. Tamme, T. Brand and C. Bahl (2007). "Solid Media Thermal Storage Development and Analysis of Modular Storage Operation Concepts for Parabolic Trough Power Plants." Journal of Solar Energy Engineering **130**(1): 011006-011006-011005.

Li, X., E. Xu, S. Song, X. Wang and G. Yuan (2017). "Dynamic simulation of two-tank indirect thermal energy storage system with molten salt." Renewable Energy **113**: 1311-1319.

LOB GmbH. (2009). "Verkstoffübersicht." Werkstoff Nr. 1.8935 Retrieved 3.5.2019, from http://www.lob-gmbh.de/de/werkstoffe/1.8935.html.

Morisson, V., M. Rady, E. Palomo and E. Arquis (2008). "Thermal energy storage systems for electricity production using solar energy direct steam generation technology." Chemical Engineering and Processing: Process Intensification **47**(3): 499-507.

Pacheco, J. E., R. W. Bradshaw, D. B. Dawson, W. De la Rosa, R. Gilbert, S. H. Goods, M. J. Hale, P. Jacobs, S. A. Jones and G. J. Kolb (2002). "Final test and evaluation results from the solar two project." Report No. SAND2002-0120, Sandia National Laboratories, Albuquerque, NM **45**.

Pelay, U., L. Luo, Y. Fan, D. Stitou and M. Rood (2017). "Thermal energy storage systems for concentrated solar power plants." Renewable and Sustainable Energy Reviews **79**: 82-100.

Prieto, C., A. Rodríguez, D. Patiño and L. F. Cabeza (2018). "Thermal energy storage evaluation in direct steam generation solar plants." Solar Energy **159**: 501-509.

Sharma, A., V. V. Tyagi, C. Chen and D. Buddhi (2009). "Review on thermal energy storage with phase change materials and applications." Renewable and Sustainable energy reviews **13**(2): 318-345.

Skinner, J. E., B. M. Brown and R. P. Selvam (2011). "Testing of High Performance Concrete as a Thermal Energy Storage Medium at High Temperatures." (54686): 723-728.

Skinner, J. E., M. N. Strasser, B. M. Brown and R. Panneer Selvam (2013). "Testing of High-Performance Concrete as a Thermal Energy Storage Medium at High Temperatures." Journal of Solar Energy Engineering **136**(2): 021004-021004-021006.

SSB. (2018). "Energibruk i industrien." Retrieved 5.4.2019.

Steinmann, W.-D. and M. Eck (2006). "Buffer storage for direct steam generation." Solar Energy **80**(10): 1277-1282.

Tamme, R., T. Bauer, J. Buschle, D. Laing, H. Müller-Steinhagen and W.-D. Steinmann (2008). "Latent heat storage above 120°C for applications in the industrial process heat sector and solar power generation." International Journal of Energy Research **32**(3): 264-271.

Unseld, M. (2015). Energiewende: VDE-Studie empfiehlt Rückkehr zur Stromheizung. https://www.vde.com/de/presse/pressemitteilungen/36-15, VDE Presse.

Yara. (2019). "Solar power molten salt." Retrieved 7.10.2019, from https://www.yara.com/chemical-and-environmental-solutions/solar-power-molten-salt/.

Zauner, C., R. Hofmann and B. Windholz (2018). Increasing Energy Efficiency in Pulp and Paper Production by Employing a New Type of Latent Heat Storage. Computer Aided Chemical Engineering. A. Friedl, J. J. Klemeš, S. Radl, P. S. Varbanov and T. Wallek, Elsevier. **43:** 1359-1364.